NORTH-HOLLAND

On Interpolating between Probability Distributions

Faruk H. Bursal

Department of Mechanical Engineering
Virginia Polytechnic Institute and State University
Blacksburg, Virginia 24061-0238

Transmitted by John Casti

ABSTRACT

Uncertainty in the simulation of physical systems is common and may be due to parameter variations or noise. When the uncertainty is random in nature, probability distributions for the quantities of interest are obtained. Sometimes, knowing only the mean and variance is sufficient; at other times, safety and reliability considerations require knowledge of the complete distribution. Computing these distributions is often a time-consuming task and needs to be repeated when some system parameters are changed. In this paper, formulas for interpolating between probability density and mass functions in spaces of arbitrary dimensionality are presented. It is found that these formulas give accurate results even when the functions one is interpolating between are not that "close." As the mesh used in interpolation is refined, the accuracy of the interpolated quantities increases; accordingly, in addition to the more complicated and robust interpolation formulas meant for the case of a coarse mesh, simplified versions that result in good accuracy when the mesh is fine are also given. Savings in computational effort up to a factor of one hundred are common even when the more complicated interpolation formulas are used. This means that interpolation is a lucrative alternative to Monte Carlo simulation and even to the Generalized Cell Mapping (GCM) method when complete probability distributions, as opposed to only the low-order statistics, are needed. It is expected that this technique will relieve much of the burden of repeated, time-consuming simulations as certain relevant parameters are varied. In addition, the given formulas may be interpreted as general-purpose algorithms for the blending of shapes, thereby leading to applications beyond what is considered in this paper.

APPLIED MATHEMATICS AND COMPUTATION 77:213–244 (1996)

655 Avenue of the Americas, New York, NY 10010
0096-3003/96/$15.00
SSDI 0096-3003(95)00216-5

1. INTRODUCTION

Uncertainty abounds in many types of analyses, and methods need to be devised that account for this uncertainty in a meaningful manner. It is only thus that the systems one designs are made as robustly reliable as possible. Uncertainty is typically assumed to be either random, leading to the study of probabilities and stochastic processes [1–4], or else due to incomplete or imprecise information, leading to the study of fuzzy sets [5, 6]. The concern in this paper is exclusively with the former. It is true that many methods have been developed over the years that aid in the analysis of evolving uncertainty; no comprehensive bibliography will be attempted here. In broad terms, existing techniques relevant to the study of dynamics with random uncertainties can be classified into those that "analytical" (including Fokker-Planck-Kolmogorov equations and their exact or approximate solution—see, for example, [1–4, 7–9]) and those which are "numerical" (including Monte Carlo simulation and the Generalized Cell Mapping method [10–15]).

The presence of nonlinearity in the equations governing a system creates problems for analysis because superposition is inapplicable and because multiple stable solutions are possible. The latter feature of nonlinear systems has led to an emphasis on global studies, which tend to be very time-consuming and costly, due to the computational effort involved. Whenever the problem at hand involves no more than simple mean and variance considerations, much work can be avoided using expedient analytical approximations such as Gaussian closure [9]. However, in general, safety and reliability considerations require more information regarding the actual extent of uncertainty and necessitate the computation of the complete probability distribution. Traditionally, Monte Carlo simulation has been the staple of such studies. However, in recent years, the method of Generalized Cell Mapping (which was originally formulated for deterministic systems) has been applied successfully to nonlinear random vibration problems, resulting in considerable savings of computational effort [10–15]. The present paper gives a more thorough account of the results presented in [16] and can be regarded as an effort in the same vein as GCM; namely, the reduction of the cost of obtaining reasonably accurate probability distributions through numerical means. Despite the original motivation of the work by the GCM method, however, the results presented are equally applicable to situations where the distributions in question have been computed using techniques other than GCM.

When a quantity that depends on some parameters is difficult to calculate, it is natural to seek to discretize the parameter space, such that values of the desired quantity for arbitrary values of the parameters may be approximated through interpolation. Recently, a related technique has been

applied to the problem of finding the probability distribution of solute concentration in an aquifer, given the probability distribution of the hydraulic conductivity [17]. To this end, conductivity values are drawn from the known distribution, and simulation is performed in order to obtain the resulting solute concentration. The functional relation between conductivity and concentration is then approximated through interpolation, leading eventually to the distribution of the concentration. Similarly, in another recent paper, certain probabilities of interest in nuclear engineering are found by interpolation based on a grid in the parameter space [18].

On a different note, interpolation has also been used to constructively *generate* approximate probability distributions [19] and reaction probabilities [20]. What appears to be absent in the existing literature, however, is a general-purpose method of interpolating between complete probability distributions (as opposed to merely individual probabilities) when certain parameters are varied. As a motivating example, consider that the usual application of the GCM method involves computing one-step transition probabilities between cells; the only difference from one cell to the next is the initial condition. It would be desirable to use initial conditions in a rather coarse grid as nodes, so that the transition probability densities from individual cells in between could be approximated through interpolation. While simple to state and attractive to contemplate, this scheme is not trivial, because one essentially needs to interpolate in function space. This paper gives the proper form of the interpolation formulas to use. A distinction is made between two spaces: the state space, on which the probability density or mass functions are supported, and the parameter space, in which the parameters that affect the outcome reside.

Sections 2 and 3 are devoted to continuous distributions described by probability density functions. In Section 2, interpolation formulas are derived for a one-dimensional parameter space. While these formulas can be regarded as specializations of the N-dimensional interpolation formulas (the subject of Section 3), they are presented first in order to explain the underlying concepts in a setting of simpler notation. Section 4 extends the formulation to discrete distributions and probability mass functions. Some examples of application are given in Section 5. Section 6 concludes the paper.

2. INTERPOLATION OF PROBABILITY DENSITY FUNCTIONS IN ONE DIMENSION

2.1 Interpolating for the Mean and Variance

As mentioned in the Introduction, the state space and the parameter space are, in general, different spaces and so can be of different dimensions. The "one dimension" in the title of this section refers to that of the

parameter space. However, in keeping with the motivation of this work by the Cell Mapping method, the following formulas are written as if the state space were identical to the parameter space (and therefore, one-dimensional as well). The reader should consult Section 3.3 for the proper interpretation if the state space and parameter space are distinct for the application at hand.

Interpolating between the ordinates corresponding to given abscissae is a commonly used procedure in numerical mathematics. The simplest possible interpolation formula is a linear interpolation between two function values. (The same formula can also be used for extrapolation, but with generally less trustworthy results.) Linear interpolation is preferred from the standpoint of simplicity and efficiency. On the other hand, if the separation of the abscissae is considerable or the function deviates significantly from being linear, the approximation errors incurred through the use of linear interpolation will be relatively large. Another option is the use of a higher-order (say, cubic) interpolation formula. For instance, Hermite cubics are frequently encountered in Finite Element analysis [21]. Although such formulas lead to marked increases in the local accuracy of the interpolation, they do so at the cost of significant complication of the interpolation formulas and their numerical evaluation. Work on the method of Interpolated Mapping has shown that, on the whole, a more densely spaced linear interpolation and a less densely spaced cubic interpolation produce results of essentially identical accuracy at the same level of computational expense [22]. Thus, the exposition in this paper is devoted exclusively to the case of linear interpolation.

Before proceeding to the more delicate issue of how probability density functions as a whole should be interpolated, it needs to be decided how the first and second-order statistics of the approximate distribution shall be determined. These, being purely numerical entities, are amenable to straightforward interpolation. Let the one-dimensional parameter be t and suppose that probability density functions of the random variable X are known for the values $t^{(0)}$ and $t^{(1)}$ of the parameter. Define the normalized interpolation coordinate α by

$$\alpha = \frac{t - t^{(0)}}{t^{(1)} - t^{(0)}}. \tag{1}$$

(It is best, though not necessary, to have $t \in [t^{(0)}, t^{(1)}]$.) Using linear interpolation and denoting by $\mu^{(0)}$ and $\mu^{(1)}$ the means of the distributions corresponding to $t^{(0)}$ and $t^{(1)}$, respectively,

$$\mu = (1 - \alpha)\mu^{(0)} + \alpha\mu^{(1)} \tag{2}$$

is found as the approximate mean corresponding to t.

For physical quantities, the mean has the same unit as X itself. The variance, on the other hand, has units of X squared. This suggests that perhaps it would be better to work with the standard deviation instead. To answer the question of whether to use linear interpolation on the variance or its square root, consider what is possibly the most purely random of all processes, the Wiener process (a model of Brownian motion) [23]. The equation governing the Wiener process is

$$\dot{X}(t) = w(t) \tag{3}$$

where $w(t)$ is Gaussian white noise. The resulting process serves as a good benchmark for stochastic dynamics because the dynamics is due entirely to the random forcing; in its absence, the solution is constant. Due to the simplicity of (3), it is possible to determine analytically the mean and variance of X as a function of time. If $w(t)$ has zero mean and a given, constant power spectral density, then the mean of X stays constant at its initial value and its variance increases linearly with time [24]. Now, notice that this process can be interpreted as a random variable parametrized by time: For each value of t, there is a well-defined distribution for X. Given distributions at two times $t^{(0)}$ and $t^{(1)}$, the variance of X at any time t is given exactly by linear interpolation between the variances at $t^{(0)}$ and $t^{(1)}$. Based on this observation, one may conclude that it is more appropriate to interpolate the variance, rather than the standard deviation, in a linear manner. Hence, using the same definition for α as before, and letting $K^{(0)}$ and $K^{(1)}$ denote the variances corresponding to $t^{(0)}$ and $t^{(1)}$,

$$K = (1 - \alpha) K^{(0)} + \alpha K^{(1)} \tag{4}$$

is obtained as the approximate variance corresponding to t. The corresponding standard deviations are defined in the usual manner as

$$\sigma = \sqrt{K}, \quad \sigma^{(0)} = \sqrt{K^{(0)}}, \quad \sigma^{(1)} = \sqrt{K^{(1)}}. \tag{5}$$

In this regard, it should be pointed out that it is not necessary to use the above-derived approximate values for the mean and variance if better estimates are computable by other means; for instance, by integration of deterministic differential equations obtained through a procedure like Gaussian closure [9, 24]. The rest of the algorithm is in no way affected by this choice.

2.2 Coordinate Transformations and Interpolation Formula

Suppose that X has the probability density functions (pdfs) $p_t(x)$, supported on the state space in which x represents a point, and parametrized

by t belonging to the parameter space. Consider two such functions to be available for values $t^{(0)}$ and $t^{(1)}$ of the parameter. It would be very convenient to interpolate between them in the naïve manner indicated by

$$p_t(x) = (1 - \alpha)\, p_{t^{(0)}}(x) + \alpha p_{t^{(1)}}(x). \tag{6}$$

Unfortunately, this is often improper, because the distributions for $t^{(0)}$ and $t^{(1)}$ will, in general, be concentrated in different regions of the state space. The result may be a bimodal distribution obtained by interpolating between two unimodal distributions. It is shown in Section 2.4 that the scheme in (6) is likely to be accurate in the limit of small separation of $\mu^{(0)}$ and $\mu^{(1)}$; otherwise, a more complicated interpolation method is required.

The essential observation is that a distribution obtained by interpolating between two distributions of comparable shape should itself exhibit that characteristic shape. The most sensible way of ensuring this outcome is to map (i.e., translate, and stretch or shrink) the pdfs so as to make the regions of the state space in which they are concentrated coincide. For instance, if the two pdfs being interpolated between exhibit the characteristic bell shape of the normal distribution, then they should be translated to place their peaks in the same location, followed by stretching or shrinking to give rise to identical spreads. This requires coordinate transformations on the arguments of the pdfs. Suppose that one wishes to obtain the approximate pdf $p_t(x)$ through interpolation. First, transformed coordinates $x^{(0)}$ and $x^{(1)}$ are defined according to

$$\frac{x - \mu}{\sigma} = \frac{x^{(0)} - \mu^{(0)}}{\sigma^{(0)}} = \frac{x^{(1)} - \mu^{(1)}}{\sigma^{(1)}}, \tag{7}$$

where all of the constants are as defined in Section 2.1. Using these transformed coordinates, the properly interpolated pdf is given by

$$p_t(x) = (1 - \alpha)\frac{dx^{(0)}}{dx} p_{t^{(0)}}(x^{(0)}) + \alpha \frac{dx^{(1)}}{dx} p_{t^{(1)}}(x^{(1)}). \tag{8}$$

The Jacobians $dx^{(0)}/dx$ and $dx^{(1)}/dx$ in this case, equal $\sigma^{(0)}/\sigma$ and $\sigma^{(1)}/\sigma$, respectively.

2.3 Verifications

It is necessary to verify that the pdf obtained through (8) exhibits the desired characteristics. First, it needs to be shown that $p_t(x)$ is a legitimate pdf. It is clear from the nature of (8) that one is interpolating linearly

between two values that are, by definition, greater than or equal to zero because $p_{t^{(0)}}(x)$ and $p_{t^{(1)}}(x)$ are pdfs. The Jacobians are also positive quantities. Therefore, $p_t(x)$ satisfies the first requirement of being a pdf; it too is greater than or equal to zero, provided that $t^{(0)} \leqslant t \leqslant t^{(1)}$ or, equivalently, $0 \leqslant \alpha \leqslant 1$. (Observe that the guarantee does not apply to extrapolation.) To complete the proof that $p_t(x)$ is a legitimate pdf, its integral over the state space must be shown to equal unity. Note that $p_{t^{(0)}}(x)$ and $p_{t^{(1)}}(x)$ already have this property since they are pdfs. Accordingly:

$$\begin{aligned}\int_{-\infty}^{\infty} p_t(x)\,dx &= (1-\alpha)\frac{dx^{(0)}}{dx}\int_{-\infty}^{\infty} p_{t^{(0)}}(x^{(0)})\,dx + \alpha\frac{dx^{(1)}}{dx}\int_{-\infty}^{\infty} p_{t^{(1)}}(x^{(1)})\,dx \\ &= (1-\alpha)\int_{-\infty}^{\infty} p_{t^{(0)}}(x^{(0)})\,dx^{(0)} + \alpha\int_{-\infty}^{\infty} p_{t^{(1)}}(x^{(1)})\,dx^{(1)} \\ &= 1-\alpha+\alpha = 1. \end{aligned} \tag{9}$$

Thus, $p_t(x)$ is seen to be a pdf. It is likewise elementary (though cumbersome) to show that $p_t(x)$ has mean μ and variance K by virtue of its construction. Observe that

$$\int_{-\infty}^{\infty} x p_{t^{(i)}}(x)\,dx = \mu^{(i)} \tag{10}$$

and

$$\int_{-\infty}^{\infty} x^2 p_{t^{(i)}}(x)\,dx = \left(\mu^{(i)}\right)^2 + K^{(i)} \tag{11}$$

for $i = 0, 1$. Solving (7) for x as a function of $x^{(0)}$ and $x^{(1)}$, one obtains

$$x = \frac{\sigma}{\sigma^{(0)}}x^{(0)} + \frac{\mu\sigma^{(0)} - \mu^{(0)}\sigma}{\sigma^{(0)}} \tag{12}$$

and

$$x = \frac{\sigma}{\sigma^{(1)}}x^{(1)} + \frac{\mu\sigma^{(1)} - \mu^{(1)}\sigma}{\sigma^{(1)}}, \tag{13}$$

hence,

$$\int_{-\infty}^{\infty} xp_t(x)\,dx = (1-\alpha)\frac{dx^{(0)}}{dx}\int_{-\infty}^{\infty} xp_{t^{(0)}}(x^{(0)})\,dx$$

$$+\,\alpha\frac{dx^{(1)}}{dx}\int_{-\infty}^{\infty} xp_{t^{(1)}}(x^{(1)})\,dx$$

$$= \frac{1-\alpha}{\sigma^{(0)}}\left[\sigma\int_{-\infty}^{\infty} x^{(0)}p_{t^{(0)}}(x^{(0)})\,dx^{(0)}\right.$$

$$\left.+\,(\mu\sigma^{(0)}-\mu^{(0)}\sigma)\int_{-\infty}^{\infty} p_{t^{(0)}}(x^{(0)})\,dx^{(0)}\right]$$

$$+\frac{\alpha}{\sigma^{(1)}}\left[\sigma\int_{-\infty}^{\infty} x^{(1)}p_{t^{(1)}}(x^{(1)})\,dx^{(1)}\right.$$

$$\left.+\,(\mu\sigma^{(1)}-\mu^{(1)}\sigma)\int_{-\infty}^{\infty} p_{t^{(1)}}(x^{(1)})\,dx^{(1)}\right]$$

$$= \frac{1-\alpha}{\sigma^{(0)}}(\mu^{(0)}\sigma+\mu\sigma^{(0)}-\mu^{(0)}\sigma)$$

$$+\frac{\alpha}{\sigma^{(1)}}(\mu^{(1)}\sigma+\mu\sigma^{(1)}-\mu^{(1)}\sigma)$$

$$= \mu(1-\alpha+\alpha) = \mu. \tag{14}$$

Proceeding similarly (with details of the algebra omitted), one obtains

$$\int_{-\infty}^{\infty} x^2 p_t(x)\,dx = (1-\alpha)\frac{dx^{(0)}}{dx}\int_{-\infty}^{\infty} x^2 p_{t^{(0)}}(x^{(0)})\,dx$$

$$+\,\alpha\frac{dx^{(1)}}{dx}\int_{-\infty}^{\infty} x^2 p_{t^{(1)}}(x^{(1)})\,dx$$

$$= (\mu^2+K)(1-\alpha+\alpha) = \mu^2+K, \tag{15}$$

i.e., $p_t(x)$ has the desired variance K. Finally, it is easily shown that when $p_{t^{(0)}}(x)$ and $p_{t^{(1)}}(x)$ describe normal distributions, then $p_t(x)$ generated

according to (8) is itself normal with mean μ and variance K. For $i = 0, 1$, one has

$$p_{t^{(i)}}(x) = \frac{1}{\sigma^{(i)}\sqrt{2\pi}} \exp\left\{ -\frac{1}{2} \frac{(x - \mu^{(i)})^2}{K^{(i)}} \right\} \tag{16}$$

as the pdf. Then, (8) can be expanded as

$$p_t(x) = (1 - \alpha) \frac{\sigma^{(0)}}{\sigma} \frac{1}{\sigma^{(0)}\sqrt{2\pi}} \exp\left\{ -\frac{1}{2} \frac{(x - \mu^{(0)})^2}{K^{(0)}} \right\}$$

$$+ \alpha \frac{\sigma^{(1)}}{\sigma} \frac{1}{\sigma^{(1)}\sqrt{2\pi}} \exp\left\{ -\frac{1}{2} \frac{(x - \mu^{(1)})^2}{K^{(1)}} \right\} \tag{17}$$

which, in light of (7), condenses to

$$p_t(x) = \frac{1}{\sigma\sqrt{2\pi}} \exp\left\{ -\frac{1}{2} \frac{(x - \mu)^2}{K} \right\}, \tag{18}$$

substantiating the assertion. More generally, whenever $p_{t^{(0)}}(x)$ and $p_{t^{(1)}}(x)$ describe distributions with the same shape, be they normal, uniform, exponential, etc., then the construction in (8) ensures that the interpolated pdf $p_t(x)$ will also have the same shape.

2.4 The Small-Separation Limit

This section is devoted to an examination of the simple interpolation formula given as (6), which is reproduced here for ease of reference:

$$p_t(x) = (1 - \alpha)\, p_{t^{(0)}}(x) + \alpha p_{t^{(1)}}(x). \tag{6}$$

It has already been mentioned that the shortcoming of this formula is its potential for yielding a distribution that is bimodal when both of the distributions being interpolated between are unimodal. An example for this occurrence is found in Section 5. First, it is clear that $p_t(x)$ thus defined is greater than or equal to zero everywhere when $0 \leqslant \alpha \leqslant 1$; furthermore, because $p_{t^{(0)}}(x)$ and $p_{t^{(1)}}(x)$ are pdfs,

$$\int_{-\infty}^{\infty} p_t(x)\, dx = (1 - \alpha) \int_{-\infty}^{\infty} p_{t^{(0)}}(x)\, dx + \alpha \int_{-\infty}^{\infty} p_{t^{(1)}}(x)\, dx$$

$$= 1 - \alpha + \alpha = 1 \tag{19}$$

and $p_t(x)$ satisfies the requirements for being a pdf. Similarly, one has

$$\int_{-\infty}^{\infty} xp_t(x)\,dx = (1-\alpha)\int_{-\infty}^{\infty} xp_{t^{(0)}}(x)\,dx + \alpha\int_{-\infty}^{\infty} xp_{t^{(1)}}(x)\,dx$$

$$= (1-\alpha)\mu^{(0)} + \alpha\mu^{(1)} = \mu, \tag{20}$$

indicating that the mean is also correctly reproduced. It is in the variance that the formula fails:

$$\int_{-\infty}^{\infty} x^2 p_t(x)\,dx = (1-\alpha)\int_{-\infty}^{\infty} x^2 p_{t^{(0)}}(x)\,dx + \alpha\int_{-\infty}^{\infty} x^2 p_{t^{(1)}}(x)\,dx$$

$$= (1-\alpha)\left(\left(\mu^{(0)}\right)^2 + K^{(0)}\right) + \alpha\left(\left(\mu^{(1)}\right)^2 + K^{(1)}\right)$$

$$= (1-\alpha)\left(\mu^{(0)}\right)^2 + \alpha\left(\mu^{(1)}\right)^2 + K, \tag{21}$$

whereas, the proper result is $\mu^2 + K$, as on the right-hand side of (15). Comparing the two, it is seen that the interpolation formula (6) results in an excess variance of

$$\Delta K = \alpha(1-\alpha)\left(\mu^{(0)} - \mu^{(1)}\right)^2. \tag{22}$$

This equation indicates that the error is of second order in the separation of the two means. Whenever $\mu^{(0)}$ and $\mu^{(1)}$ are relatively close (which is likely when $t^{(0)}$ and $t^{(1)}$ are close), one may use (6) as a shortcut without sacrificing accuracy, at least to second order. Examples are provided in Section 5. As a rough criterion, it is suggested to use the simplified interpolation formula when $(\Delta\mu)^2 \ll K$, where $\Delta\mu = \mu^{(0)} - \mu^{(1)}$.

3. INTERPOLATION OF PROBABILITY DENSITY FUNCTIONS IN N DIMENSIONS

3.1 Interpolation Formulas

In this section, the formulas of Section 2 are generalized to the case of an N-dimensional parameter space. As was done in Section 2, it is assumed for the time being that the state space and the parameter space are of identical dimension; the very minor changes that occur when this is not the case are discussed in Section 3.3.

To begin with, the definition of the normalized interpolation coordinate needs to be updated. Consider that the parameter t is now a vector $\mathbf{t}$, with elements t_i, $i = 1, \ldots, N$. Analogously to the interval $[t^{(0)}, t^{(1)}]$ that bounded t in the one-dimensional case, it is possible to define a hypercube in N dimensions that is the product of N such intervals and bounds $\mathbf{t}$. This hypercube has 2^N vertices, which may be labeled using N-tuples consisting of the digits 0 and 1. For example, the corners of a rectangle in two dimensions would receive the designations $(0, 0)$, $(0, 1)$, $(1, 0)$ and $(1, 1)$, in analogy to the endpoints of the interval in one dimension being labeled 0 and 1. Figure 1 illustrates the labeling; the extension to higher dimensions should be obvious. The parameter vectors corresponding to the vertices are accordingly superscripted with these labels. Subsequently, the following normalized interpolation coordinates are defined:

$$\alpha_i = \frac{t_i - t_i^{(0,0,\ldots,0)}}{t_i^{(0,0,\ldots,1,\ldots,0)} - t_i^{(0,0,\ldots,0)}} \tag{23}$$

where the "1" in the denominator occurs at the i-th position in the N-tuple. In the 2-dimensional example, one would have

$$\alpha_1 = \frac{t_1 - t_1^{(0,0)}}{t_1^{(1,0)} - t_1^{(0,0)}} \tag{24}$$

and

$$\alpha_2 = \frac{t_2 - t_2^{(0,0)}}{t_2^{(0,1)} - t_2^{(0,0)}}. \tag{25}$$

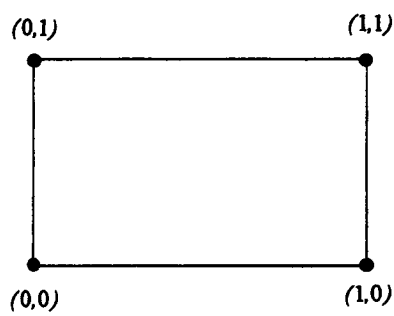

FIG. 1. Labeling of nodes in two dimensions.

The linear interpolation functions to use are

$$f^{(0)}(\alpha) = 1 - \alpha,$$
$$f^{(1)}(\alpha) = \alpha. \tag{26}$$

In terms of these interpolation coordinates and functions, the following identity is provided to introduce the notation used:

$$\mathbf{t} = \sum_{i_1, \ldots, i_N = 0}^{1} f^{(i_1)}(\alpha_1) \cdots f^{(i_N)}(\alpha_N)\mathbf{t}^{(i_1, \ldots, i_N)}. \tag{27}$$

There are a total of 2^N terms in the above sum. One may visualize the indices $i_1, \ldots, i_N$ as executing nested loops to produce the final result. The expanded version of (27) in two dimensions is

$$\mathbf{t} = (1 - \alpha_1)(1 - \alpha_2)\mathbf{t}^{(0,0)} + (1 - \alpha_1)\alpha_2\mathbf{t}^{(0,1)} + \alpha_1(1 - \alpha_2)\mathbf{t}^{(1,0)} + \alpha_1\alpha_2\mathbf{t}^{(1,1)}. \tag{28}$$

Let $\mu^{(0,0,\ldots,0)}$ be the mean of the distribution corresponding to the parameter vector $\mathbf{t}^{(0,0,\ldots,0)}$, and so on up to $\mu^{(1,1,\ldots,1)}$; and let μ denote the mean for $\mathbf{t}$. Then, the linear approximation to μ is given by

$$\mu = \sum_{i_1, \ldots, i_N = 0}^{1} f^{(i_1)}(\alpha_1) \cdots f^{(i_N)}(\alpha_N)\mu^{(i_1, \ldots, i_N)}. \tag{29}$$

Similarly, with $\mathbf{K}^{(0,0,\ldots,0)}, \ldots$ denoting the covariance matrices corresponding to the same parameter vectors, one has

$$\mathbf{K} = \sum_{i_1, \ldots, i_N = 0}^{1} f^{(i_1)}(\alpha_1) \cdots f^{(i_N)}(\alpha_N)\mathbf{K}^{(i_1, \ldots, i_N)} \tag{30}$$

as the approximate covariance matrix for $\mathbf{t}$. As in the case of interpolation in one dimension, one may use a different method for computing the mean and covariance corresponding to $\mathbf{t}$ when feasible; the rest of the algorithm remains unaffected. The coordinate transformations to use are given by

$$\sqrt{\mathbf{K}^{-1}}(\mathbf{x} - \mu) = \sqrt{\mathbf{K}^{(i_1, \ldots, i_N)^{-1}}}(\mathbf{x}^{(i_1, \ldots, i_N)} - \mu^{(i_1, \ldots, i_N)}) \quad i_1, \ldots, i_N = 0, 1 \tag{31}$$

or, equivalently, by

$$\mathbf{x}^{(i_1,\ldots,i_N)} = \sqrt{\mathbf{K}^{(i_1,\ldots,i_N)}\mathbf{K}^{-1}}\,(\mathbf{x} - \boldsymbol{\mu}) + \boldsymbol{\mu}^{(i_1,\ldots,i_N)} \qquad i_1,\ldots,i_N = 0,1. \tag{32}$$

The Jacobian of each transformation is expressed as

$$J^{(i_1,\ldots,i_N)} = \sqrt{\det(\mathbf{K}^{(i_1,\ldots,i_N)}\mathbf{K}^{-1})} \qquad i_1,\ldots,i_N = 0,1. \tag{33}$$

Now consider that a known pdf $p_{\mathbf{t}^{(i_1,\ldots,i_N)}}(x)$ corresponds to each parameter vector $\mathbf{t}^{(i_1,\ldots,i_N)}$, and recall that $\mathbf{t}^{(i_1,\ldots,i_N)}$ constitute the 2^N vertices of a hypercube bounding $\mathbf{t}$ in the parameter space. With all of the above definitions, the final interpolation formula for the desired pdf corresponding to $\mathbf{t}$ is

$$p_{\mathbf{t}}(\mathbf{x}) = \sum_{i_1,\ldots,i_N=0}^{1} f^{(i_1)}(\alpha_1)\cdots f^{(i_N)}(\alpha_N)\, J^{(i_1,\ldots,i_N)} p_{\mathbf{t}^{(i_1,\ldots,i_N)}}(\mathbf{x}^{(i_1,\ldots,i_N)}). \tag{34}$$

As in the one-dimensional case, there exists a simplified (but less accurate, as is shown in Section 3.2) interpolation formula given by

$$p_{\mathbf{t}}(\mathbf{x}) = \sum_{i_1,\ldots,i_N=0}^{1} f^{(i_1)}(\alpha_1)\cdots f^{(i_N)}(\alpha_N)\, p_{\mathbf{t}^{(i_1,\ldots,i_N)}}(\mathbf{x}). \tag{35}$$

Defining by $\Delta\boldsymbol{\mu}$ the difference in the means of any two distributions selected from those corresponding to $\mathbf{t}^{(i_1,\ldots,i_N)}$, it is suggested to use the simpler formula when $\max(\Delta\boldsymbol{\mu}^{\mathrm{T}}\Delta\boldsymbol{\mu}) \ll \det\mathbf{K}$; i.e., when the difference of the means is relatively small.

3.2 Verifications

Due to the linear change of variables in (31), various integrals involving $p_{\mathbf{t}}(\mathbf{x})$ in N dimensions have the correct values, echoing the one-dimensional

results in Section 2.3. In particular,

$$\int_{-\infty}^{\infty} \cdots \int_{-\infty}^{\infty} p_t(\mathbf{x})\, dx_1 \cdots dx_N$$

$$= \sum_{i_1, \ldots, i_N = 0}^{1} f^{(i_1)}(\alpha_1) \cdots f^{(i_N)}(\alpha_N)\, J^{(i_1, \ldots, i_N)}$$

$$\cdot \left\{ \int_{-\infty}^{\infty} \cdots \int_{-\infty}^{\infty} p_{t^{(i_1, \ldots, i_N)}}(\mathbf{x}^{(i_1, \ldots, i_N)})\, dx_1 \cdots dx_N \right\}$$

$$= \sum_{i_1, \ldots, i_N = 0}^{1} f^{(i_1)}(\alpha_1) \cdots f^{(i_N)}(\alpha_N)$$

$$\cdot \left\{ \int_{-\infty}^{\infty} \cdots \int_{-\infty}^{\infty} p_{t^{(i_1, \ldots, i_N)}}(\mathbf{x}^{(i_1, \ldots, i_N)})\, dx_1^{(i_1, \ldots, i_N)} \cdots dx_N^{(i_1, \ldots, i_N)} \right\}$$

$$= \sum_{i_1, \ldots, i_N = 0}^{1} f^{(i_1)}(\alpha_1) \cdots f^{(i_N)}(\alpha_N) = 1 \tag{36}$$

holds and; because all terms in the sum in (34) are greater than or equal to zero for $0 \leqslant \alpha_i \leqslant 1$, $i = 1, \ldots, N$; $p_t(\mathbf{x})$ satisfies the requirements for being a legitimate pdf. Furthermore, one can show (using straightforward algebraic manipulations whose details will be omitted) that

$$\int_{-\infty}^{\infty} \cdots \int_{-\infty}^{\infty} \mathbf{x}\, p_t(\mathbf{x})\, dx_1 \cdots dx_N$$

$$= \sum_{i_1, \ldots, i_N = 0}^{1} f^{(i_1)}(\alpha_1) \cdots f^{(i_N)}(\alpha_N)\, J^{(i_1, \ldots, i_N)}$$

$$\cdot \left\{ \int_{-\infty}^{\infty} \cdots \int_{-\infty}^{\infty} \mathbf{x}\, p_{t^{(i_1, \ldots, i_N)}}(\mathbf{x}^{(i_1, \ldots, i_N)})\, dx_1 \cdots dx_N \right\}$$

$$= \mu \left\{ \sum_{i_1, \ldots, i_N = 0}^{1} f^{(i_1)}(\alpha_1) \cdots f^{(i_N)}(\alpha_N) \right\} = \mu \tag{37}$$

and

$$\int_{-\infty}^{\infty} \cdots \int_{-\infty}^{\infty} \mathbf{x}\mathbf{x}^{\mathrm{T}} p_t(\mathbf{x})\, dx_1 \cdots dx_N$$

$$= \sum_{i_1, \ldots, i_N = 0}^{1} f^{(i_1)}(\alpha_1) \cdots f^{(i_N)}(\alpha_N)\, J^{(i_1, \ldots, i_N)}$$

$$\cdot \left\{ \int_{-\infty}^{\infty} \cdots \int_{-\infty}^{\infty} \mathbf{x}\mathbf{x}^{\mathrm{T}} p_{t^{(i_1, \ldots, i_N)}}(\mathbf{x}^{(i_1, \ldots, i_N)})\, dx_1 \cdots dx_N \right\}$$

$$= (\mu\mu^{\mathrm{T}} + \mathbf{K}) \left\{ \sum_{i_1, \ldots, i_N = 0}^{1} f^{(i_1)}(\alpha_1) \cdots f^{(i_N)}(\alpha_N) \right\}$$

$$= \mu\mu^{\mathrm{T}} + \mathbf{K}, \tag{38}$$

i.e., $p_t(\mathbf{x})$ has the desired statistics up to second order. Also, when all of the distributions $p_{t^{(i_1, \ldots, i_N)}}(\mathbf{x})$ are normal, then $p_t(\mathbf{x})$ constructed according to (34) is also normal, as can be seen below:

$$p_t(\mathbf{x}) = \sum_{i_1, \ldots, i_N = 0}^{1} f^{(i_1)}(\alpha_1) \cdots f^{(i_N)}(\alpha_N)\, J^{(i_1, \ldots, i_N)} \frac{1}{\sqrt{(2\pi)^N \det \mathbf{K}^{(i_1, \ldots, i_N)}}}$$

$$\cdot \exp\left\{ -\frac{1}{2} \left(\mathbf{x}^{(i_1, \ldots, i_N)} - \mu^{(i_1, \ldots, i_N)}\right)^{\mathrm{T}} \right.$$

$$\left. \times \mathbf{K}^{(i_1, \ldots, i_N)^{-1}} \left(\mathbf{x}^{(i_1, \ldots, i_N)} - \mu^{(i_1, \ldots, i_N)}\right) \right\}$$

$$= \sum_{i_1, \ldots, i_N = 0}^{1} f^{(i_1)}(\alpha_1) \cdots$$

$$f^{(i_N)}(\alpha_N) \frac{1}{\sqrt{(2\pi)^N \det \mathbf{K}}} \exp\left\{ -\frac{1}{2} (\mathbf{x} - \mu)^{\mathrm{T}} \mathbf{K}^{-1} (\mathbf{x} - \mu) \right\}$$

$$= \frac{1}{\sqrt{(2\pi)^N \det \mathbf{K}}} \exp\left\{ -\frac{1}{2} (\mathbf{x} - \mu)^{\mathrm{T}} \mathbf{K}^{-1} (\mathbf{x} - \mu) \right\}. \tag{39}$$

The same situation occurs whenever all of the distributions $p_{\mathbf{t}(i_1,\ldots,i_N)}(\mathbf{x})$ have a common characteristic shape and differ only in scaling; the resulting interpolated distribution $p_{\mathbf{t}}(\mathbf{x})$ exhibits the same shape.

The simplified interpolation formula in (35), like its one-dimensional counterpart, passes the tests for being a legitimate pdf and reproducing the desired mean, as is easily seen:

$$\begin{aligned}\int_{-\infty}^{\infty}\cdots\int_{-\infty}^{\infty} p_{\mathbf{t}}(\mathbf{x})\,dx_1\cdots dx_N &= \sum_{i_1,\ldots,i_N=0}^{1} f^{(i_1)}(\alpha_1)\cdots f^{(i_N)}(\alpha_N)\\ &\quad\cdot\left\{\int_{-\infty}^{\infty}\cdots\int_{-\infty}^{\infty} p_{\mathbf{t}(i_1,\ldots,i_N)}(\mathbf{x})\,dx_1\cdots dx_N\right\}\\ &= \sum_{i_1,\ldots,i_N=0}^{1} f^{(i_1)}(\alpha_1)\cdots f^{(i_N)}(\alpha_N) = 1, \quad (40)\end{aligned}$$

$$\begin{aligned}&\int_{-\infty}^{\infty}\cdots\int_{-\infty}^{\infty}\mathbf{x}\,p_{\mathbf{t}}(\mathbf{x})\,dx_1\cdots dx_N\\ &\quad= \sum_{i_1,\ldots,i_N=0}^{1} f^{(i_1)}(\alpha_1)\cdots f^{(i_N)}(\alpha_N)\\ &\qquad\cdot\left\{\int_{-\infty}^{\infty}\cdots\int_{-\infty}^{\infty}\mathbf{x}\,p_{\mathbf{t}(i_1,\ldots,i_N)}(\mathbf{x})\,dx_1\cdots dx_N\right\}\\ &\quad= \sum_{i_1,\ldots,i_N=0}^{1} f^{(i_1)}(\alpha_1)\cdots f^{(i_N)}(\alpha_N)\,\mu^{(i_1,\ldots,i_N)} = \mu. \quad (41)\end{aligned}$$

However, the formula leads to an excess covariance, because

$$\begin{aligned}&\int_{-\infty}^{\infty}\cdots\int_{-\infty}^{\infty}\mathbf{x}\mathbf{x}^{\mathrm{T}}p_{\mathbf{t}}(\mathbf{x})\,dx_1\cdots dx_N\\ &\quad= \sum_{i_1,\ldots,i_N=0}^{1} f^{(i_1)}(\alpha_1)\cdots f^{(i_N)}(\alpha_N)\\ &\qquad\cdot\left\{\int_{-\infty}^{\infty}\cdots\int_{-\infty}^{\infty}\mathbf{x}\mathbf{x}^{\mathrm{T}}p_{\mathbf{t}(i_1,\ldots,i_N)}(\mathbf{x})\,dx_1\cdots dx_N\right\}\\ &\quad= \sum_{i_1,\ldots,i_N=0}^{1}\left\{f^{(i_1)}(\alpha_1)\cdots f^{(i_N)}(\alpha_N)\,\mu^{(i_1,\ldots,i_N)}\mu^{(i_1,\ldots,i_N)^{\mathrm{T}}}\right\} + \mathbf{K}\\ &\quad\neq \mu\mu^{\mathrm{T}} + \mathbf{K}. \quad (42)\end{aligned}$$

It is therefore suggested that this simpler formula be used only when the means of the distributions being interpolated between do not differ appreciably in comparison with the covariance $\mathbf{K}$.

3.3 Accounting for Separate Parameter and State Spaces

The formulas up to this point have been presented as if the parameter space and the state space were identical; however, they apply equally well when that is not the case. Note that the following discussion applies in general and includes the cases of a one-dimensional parameter space or state space as well.

The dimension of the parameter space governs the number of nodal values that must be present for interpolation. As discussed in Section 3.1, a hypercube with 2^N vertices bounds the parameter vector $\mathbf{t}$ in N-dimensional space. The resulting normalized interpolation coordinates, interpolation functions, and overall interpolation formula are as given in (23), (26), and (27), regardless of the dimension of the state space. The coordinate transformations in (31), the corresponding Jacobians in (33), and the final pdf interpolation formula in (34) are likewise formally independent of the state space dimension N_S. The only quantities that N_S has any effect on are the mean vector $\boldsymbol{\mu}$ and the covariance matrix $\mathbf{K}$; they are N_S by 1 and N_S by N_S, respectively. Accordingly, the computations involved in evaluating the various Jacobians, etc., will require an effort dependent on N_S.

In addition, the integrals used in Section 3.2 for verifying various properties of the interpolated pdf need to be rewritten when $N_S \neq N$; for instance, an infinitesimal volume element in the state space is now $dx_1 \cdots dx_{N_S}$. This is simply a matter of bookkeeping and does not in any way affect the validity of the results presented.

4. INTERPOLATION OF PROBABILITY MASS FUNCTIONS

4.1 Definition and Motivation Via Cell Mappings

A probability mass function (pmf), sometimes referred to simply as "probability function," is the discrete analog of the continuous pdf. Where the properties of the pdf are defined in terms of integrals, corresponding properties of the pmf are defined in terms of summations. Pmfs apply when the random variable $\mathbf{X}$ assumes values $\mathbf{x}_j$, $j = 1, 2, \ldots$, with associated probabilities $P(\mathbf{x}_j)$, denoted $P(j)$ henceforth. The range of j may be finite or infinite. It is understood that $P(j) \geqslant 0$ for all j; furthermore, the following normalization condition must be satisfied:

$$\sum_j P(j) = 1. \tag{43}$$

The notion of a discrete random variable is too general for a satisfactory interpolation scheme to be devised. Therefore, in what follows, $\mathbf{x}_j$ are restricted to uniform "cells," in keeping with the Cell Mapping technique. Cells are subentities into which the state space has been divided. They are nonoverlapping and collectively cover the entire state space of interest. When the state space is infinite in extent, cells lying outside a chosen region are often lumped into a single "sink cell" for the purpose of keeping the number of cells finite. The formulas presented in this section are written under the assumption of an infinite state space, but the user may decide to lump cells together by summing their associated probabilities at the end.

The concept of a cell state space was originally motivated by the impossibility of measuring continuous variables with unlimited precision. Thus, a cell state space with its probability structure in terms of a pmf can be interpreted as an approximation to a continuous state space with an associated pdf. In other instances, the distribution can be discrete by nature. What matters for the development in this paper is that the given pmf correspond to a *uniform* array of cells in the state space, regardless of its particular interpretation. In those instances where $\mathbf{X}$ truly takes on discrete values $\mathbf{x}_j$, cells of equal size must be artificially defined around those values. The formulas presented in the remainder of this section are written using C_j to denote the cell numbered j, with center point $\mathbf{x}_j$ and total associated probability $P(j)$. The range of j is left unspecified and assumed to be infinite in theory. In practice, it may be limited to those cells for which $P(j)$ is greater than some chosen threshold.

4.2 Interpolating for the Second-Order Statistics

Let N denote the dimension of the parameter space as usual. It is assumed that the parameter space is continuous for purposes of interpolation; only the state space has the cellular structure. The parameter vector $\mathbf{t}$ is bounded by the same N-dimensional hypercube described in Section 3, with $\mathbf{t}^{(i_1,\ldots,i_N)}$ as the parameter vectors at the vertices. There corresponds a given pmf $P_{\mathbf{t}^{(i_1,\ldots,i_N)}}(j)$ to each of the $\mathbf{t}^{(i_1,\ldots,i_N)}$, and the pmf $P_{\mathbf{t}}(j)$ corresponding to $\mathbf{t}$ is desired. The statistics of the distributions up to second order are given by

$$\boldsymbol{\mu}^{(i_1,\ldots,i_N)} = \sum_j \mathbf{x}_j^{(i_1,\ldots,i_N)} P_{\mathbf{t}^{(i_1,\ldots,i_N)}}(j) \tag{44}$$

and

$$\mathbf{K}^{(i_1,\ldots,i_N)} = \sum_j \left(\mathbf{x}_j^{(i_1,\ldots,i_N)} - \boldsymbol{\mu}^{(i_1,\ldots,i_N)}\right) \times \left(\mathbf{x}_j^{(i_1,\ldots,i_N)} - \boldsymbol{\mu}^{(i_1,\ldots,i_N)}\right)^{\mathrm{T}} P_{\mathbf{t}^{(i_1,\ldots,i_N)}}(j). \tag{45}$$

It is emphasized that the cell state space is the *same* for all of the distributions; it is only in the $P(j)$ that differences exist.

If the cells have been defined by lumping the probabilities resident in macroscopic regions of an underlying continuous state space, the resulting values for μ and $\mathbf{K}$ as given by (44) and (45) will, in general, differ somewhat from their continuous counterparts. This is an unavoidable consequence of casting the problem in discrete form; however, with small enough cells, the differences will be negligible. If the mean and covariance of the continuously distributed variable are available, they should be used, as they will lead to more accurate results. In any event, the approximate mean μ and covariance $\mathbf{K}$ corresponding to $\mathbf{t}$ are given by (29) and (30) in Section 3.1.

4.3 Coordinate Transformations and Interpolation Formula

All distributions are defined on the same cellular state space and individually have the property that

$$\sum_j P_{\mathbf{t}^{(i_1,\ldots,i_N)}}(j) = 1. \tag{46}$$

Accordingly, the required coordinate transformations must be performed with care. It is possible to define them in the same manner as before, namely, using (31) in Section 3.1. For the present purposes, it is more advantageous to rewrite (31) in terms of the inverse transformation, namely,

$$\mathbf{x} = \sqrt{\mathbf{K}\mathbf{K}^{(i_1,\ldots,i_N)^{-1}}}\left(\mathbf{x}^{(i_1,\ldots,i_N)} - \mu^{(i_1,\ldots,i_N)}\right) + \mu \qquad i_1,\ldots,i_N = 0,1. \tag{47}$$

However, regardless of the particular form used, this procedure does not map a cell center $\mathbf{x}_j$ to some other $\mathbf{x}_k$; indeed, it does not map cell C_j to C_k in any meaningful sense, even though the transformation is affine. As an example, Figure 2 shows a uniform grid before application of (47), and its appearance after the coordinate transformation. In order to account for the lack of a one-to-one correspondence between cells in the two grids, quantities $\gamma_{jk}^{(i_1,\ldots,i_N)}$ designating "volume fractions" must be defined as indicated below:

$$\gamma_{jk}^{(i_1,\ldots,i_N)} = \text{fraction of the volume of deformed cell } k \text{ in undeformed cell } j. \tag{48}$$

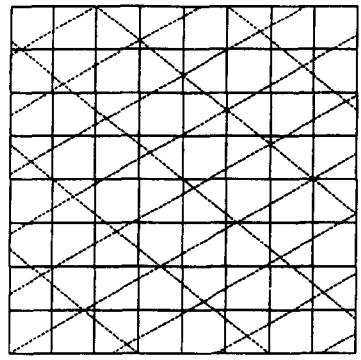

FIG. 2. Deformed grid superimposed on undeformed grid.

Here, "undeformed" refers to the original grid of cells, and "deformed" refers to the same grid skewed under the coordinate transformation in (47) and superimposed on the original grid, as in Figure 2. From the definition in (48), a normalization relation is readily apparent:

$$\sum_j \gamma_{jk}^{(i_1,\ldots,i_N)} = 1. \tag{49}$$

Furthermore, accounting for the fact that the cell volumes in the deformed and undeformed grids are different, one has

$$\sum_k \gamma_{jk}^{(i_1,\ldots,i_N)} = J^{(i_1,\ldots,i_N)} \tag{50}$$

where the Jacobian is as given in (33). In terms of the volume fractions, the overall interpolation formula for the desired pmf is given by

$$P_t(j) = \sum_{i_1,\ldots,i_N=0}^{1} f^{(i_1)}(\alpha_1)\cdots f^{(i_N)}(\alpha_N)\left\{\sum_k \gamma_{jk}^{(i_1,\ldots,i_N)} P_{t^{(i_1,\ldots,i_N)}}(k)\right\}. \tag{51}$$

When the parameter space is one-dimensional, the formula becomes

$$P_t(j) = (1-\alpha)\left\{\sum_k \gamma_{jk}^{(0)} P_{t^{(0)}}(k)\right\} + \alpha\left\{\sum_k \gamma_{jk}^{(1)} P_{t^{(1)}}(k)\right\}. \tag{52}$$

The range of k is theoretically infinite in the above equations; however, no contribution to the sums will result from $P_{\mathbf{t}^{(i_1,\ldots,i_N)}}(k)$ that are zero. More practically, when the $P_{\mathbf{t}^{(i_1,\ldots,i_N)}}(k)$ become smaller than the desired precision, the sums may be terminated. The meaningful range of j is dictated by the region of interest. The simplified version of (51), to be used only in the case of small nodal separation, is

$$P_t(j) = (1-\alpha)\, P_{t^{(0)}}(j) + \alpha P_{t^{(1)}}(j). \tag{53}$$

4.4 Verifications

Due to the property of the volume fractions $\gamma_{jk}^{(i_1,\ldots,i_N)}$ given in (50), they can be regarded as the discrete equivalent of the Jacobians used in the continuous interpolation formula (34). In essence, because the coordinate transformations (47) do not map cells to each other in a one-to-one manner, the probability resident in a cell prior to deformation must be divided up among several cells after deformation. This is accomplished by using the volume fractions as the guide to the probability allocation. While this scheme is particularly simple and perhaps obvious, it is not the only sensible one; as can be seen below, any set of $\gamma_{jk}^{(i_1,\ldots,i_N)}$ with the normalization property in (49) will lead to the desired result of $\sum_j P_{\mathbf{t}}(j) = 1$:

$$\begin{aligned}
\sum_j P_{\mathbf{t}}(j) &= \sum_{i_1,\ldots,i_N=0}^{1} f^{(i_1)}(\alpha_1)\cdots f^{(i_N)}(\alpha_N) \sum_j \left\{\sum_k \gamma_{jk}^{(i_1,\ldots,i_N)} P_{\mathbf{t}^{(i_1,\ldots,i_N)}}(k)\right\} \\
&= \sum_{i_1,\ldots,i_N=0}^{1} f^{(i_1)}(\alpha_1)\cdots f^{(i_N)}(\alpha_N) \sum_k P_{\mathbf{t}^{(i_1,\ldots,i_N)}}(k) \sum_j \gamma_{jk}^{(i_1,\ldots,i_N)} \\
&= \sum_{i_1,\ldots,i_N=0}^{1} f^{(i_1)}(\alpha_1)\cdots f^{(i_N)}(\alpha_N) \sum_k P_{\mathbf{t}^{(i_1,\ldots,i_N)}}(k) \\
&= \sum_{i_1,\ldots,i_N=0}^{1} f^{(i_1)}(\alpha_1)\cdots f^{(i_N)}(\alpha_N) = 1.
\end{aligned} \tag{54}$$

However, with the "volume fraction" definition of the $\gamma_{jk}^{(i_1,\ldots,i_N)}$, the overall mean is not quite correctly reproduced because

$$\begin{aligned}
\sum_j \mathbf{x}_j P_{\mathbf{t}}(j) &= \sum_{i_1,\ldots,i_N=0}^{1} f^{(i_1)}(\alpha_1)\cdots f^{(i_N)}(\alpha_N) \\
&\quad \times \sum_j \mathbf{x}_j \left\{ \sum_k \gamma_{jk}^{(i_1,\ldots,i_N)} P_{\mathbf{t}^{(i_1,\ldots,i_N)}}(k) \right\} \\
&= \sum_{i_1,\ldots,i_N=0}^{1} f^{(i_1)}(\alpha_1)\cdots f^{(i_N)}(\alpha_N) \\
&\quad \times \sum_k P_{\mathbf{t}^{(i_1,\ldots,i_N)}}(k) \sum_j \mathbf{x}_j \gamma_{jk}^{(i_1,\ldots,i_N)} \\
&\neq \sum_{i_1,\ldots,i_N=0}^{1} f^{(i_1)}(\alpha_1)\cdots f^{(i_N)}(\alpha_N) \sum_k \mathbf{x}_k P_{\mathbf{t}^{(i_1,\ldots,i_N)}}(k) \\
&= \sum_{i_1,\ldots,i_N=0}^{1} f^{(i_1)}(\alpha_1)\cdots f^{(i_N)}(\alpha_N)\mu^{(i_1,\ldots,i_N)} = \mu. \qquad (55)
\end{aligned}$$

This is yet another consequence of the macroscopic cell size which, as indicated in Section 4.2, causes the discrete mean and covariance to differ from their continuous versions. It is possible in this instance to eliminate the difference between the mean of the interpolated distribution and that used in defining the coordinate transformations (47). However, in light of the fact that the latter is likely inexact to begin with, the added effort of re-defining the $\gamma_{jk}^{(i_1,\ldots,i_N)}$ to ensure $\Sigma_j \mathbf{x}_j \gamma_{jk}^{(i_1,\ldots,i_N)} = \mathbf{x}_k$ (and thereby, $\Sigma_j \mathbf{x}_j P_{\mathbf{t}}(j) = \mu$) appears ill-advised. In practice, the differences in question shrink rapidly with cell size and effectively become zero to within tolerance.

Likewise, the volume fractions themselves need not be computed exactly to obtain results of acceptable precision; a simple, yet effective algorithm is to place a number of "test points" in the undeformed cell and observe which cells they fall into upon deformation. Then, by counting the number that fall into different cells and dividing by the total number of test points used, approximations to the $\gamma_{jk}^{(i_1,\ldots,i_N)}$ with the built-in property (49) can be obtained. This algorithm is suggested by the scheme used in the Generalized Cell Mapping method for computing transition probabilities between cells [11].

5. SOME EXAMPLES OF APPLICATION

5.1 Application to Probability Density Functions

The method is illustrated on a sample problem taken from [15]. This example is instructive, due to the availability of the exact steady-state pdf as a function of various parameters but is not otherwise special with regard to the new method; other examples that were studied led to comparable results. The system is question is governed by

$$\dot{x} + \alpha x + \beta x^3 = w(t) \tag{56}$$

where $w(t)$ is a Gaussian white noise process with $E[w(t)] = 0$ and $E[w(t)w(t')] = 2D_w\delta(t - t')$. The exact steady-state pdf of x can be found [15] as

$$p_s(x) = C\exp\left\{-\frac{1}{2D_w}\left(\alpha x^2 + \frac{1}{2}\beta x^4\right)\right\}, \tag{57}$$

where C is a normalization constant. This distribution is the one attained as $t \to \infty$, regardless of the initial distribution. However, intermediate distributions can differ considerably from the steady state. In fact, it can be shown [15] that $p(x, \tau | x_0, 0)$ (the pdf of x at time τ, given that x equals x_0 with probability one at time 0) is approximately Gaussian when τ is sufficiently small. The meaning of the latter is rather vague, but $\tau \leqslant 0.5$ appears to be sufficiently small for this problem. Accordingly, interpolation is now attempted on short-time Gaussian pdfs with $\tau = 0.5$. In Figure 3, pdfs corresponding to $x_0 = 0$ and $x_0 = 1$ are shown with dotted lines; x_0 in this instance serves as the one-dimensional parameter for interpolation purposes. The other parameters in (56) have been set to their nominal values of $\alpha = -1$, $\beta = 2$ and $D_w = 0.1$. The exact pdf corresponding to $x_0 = 0.25$ is shown as the solid curve. The dotted curve is the pdf interpolated using the "proper" formula in (8), while the dash-dot curve is the pdf obtained through the simplified formula (6). It can be seen that the latter leads to an apparent bimodal distribution due to the significant difference in the means of the two dotted pdfs. No such problem occurs when the proper interpolation formula is used. The shape is almost exact, as is (accordingly) the variance; the mean, on the other hand, is somewhat off. Indeed, it appears from numerous tests of the method that linear interpolation for the mean is often the most significant contributor to errors. This suggests that a higher-order interpolation might be advisable; however, no such attempt has been made in this paper. Figure 4 is similar in every way to Figure 3 except for the considerably smaller separation of $x_0 = 0$ and $x_0 = 0.14$ in the

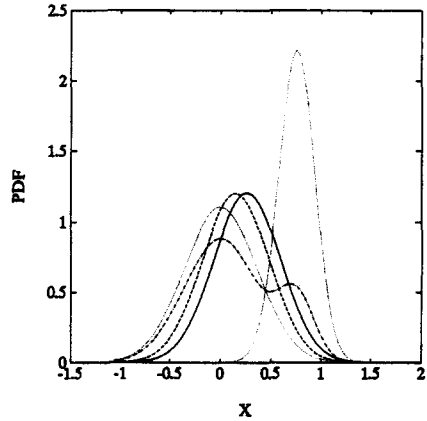

FIG. 3. Pdfs for $\alpha = -1$, $\beta = 2$, $D_w = 0.1$, and $t = 0.5$. Dotted: Exact pdfs for $x_0 = 0$ and $x_0 = 1$, Solid: Exact pdf for $x_0 = 0.25$, Dashed: Approximate pdf for $x_0 = 0.25$ using (6), Dash-dot: Approximate pdf for $x_0 = 0.25$ using (7).

parameter space. It can be seen that the interpolated pdfs are now in close agreement with the exact pdf.

After these observations on the transient behavior, interpolation of the steady-state pdfs is now illustrated with several examples. The noise intensity is fixed at $D_w = 0.1$. First, in Figure 5, exact pdfs for $\alpha = -0.5$ (dashed) and $\alpha = -1.5$ (solid) are shown, with the other parameter fixed at

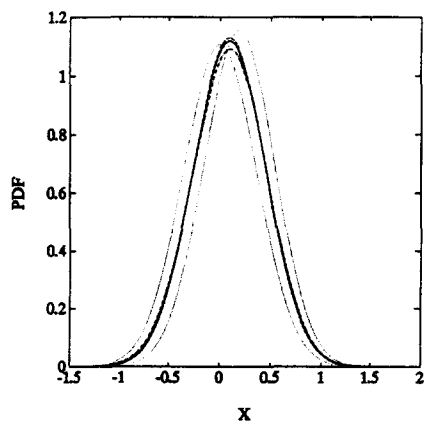

FIG. 4. Pdfs for $\alpha = -1$, $\beta = 2$, $D_w = 0.1$, and $t = 0.5$. Dotted: Exact pdfs for $x_0 = 0$ and $x_0 = 0.14$, Solid: Exact pdf for $x_0 = 0.07$, Dashed: Approximate pdf for $x_0 = 0.07$ using (6), Dash-dot: Approximate pdf for $x_0 = 0.07$ using (7).

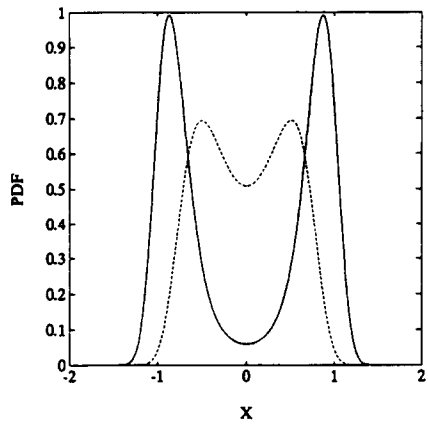

FIG. 5. Exact steady-state pdfs for $\beta = 2$ and $D_w = 0.1$. Solid: $\alpha = -1.5$, Dashed: $\alpha = -0.5$.

$\beta = 2$. Likewise, Figure 6 depicts exact pdfs with $\alpha = -1$ kept fixed, and β successively set to 1.5 (dashed) and 2.5 (solid). The pdf corresponding to $\alpha = -1$ and $\beta = 2$ is the one desired. The solid curve in Figure 7 shows the exact pdf for those values of the parameters. Superimposed on the same plot are the approximate pdfs obtained through the proper formula (8), shown as a dashed curve, and through the simplified formula (6), shown as a dash-dot curve. These have been obtained by interpolating between the pdfs shown in

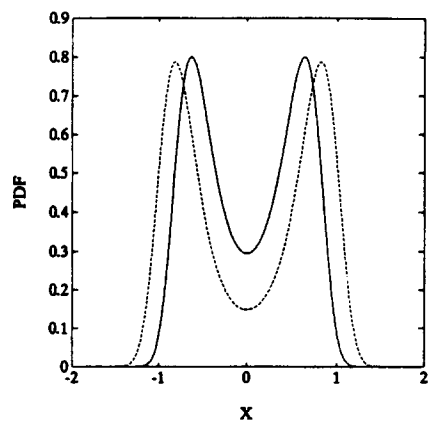

FIG. 6. Exact steady-state pdfs for $\alpha = -1$ and $D_w = 0.1$. Solid: $\beta = 2.5$, Dashed: $\beta = 1.5$.

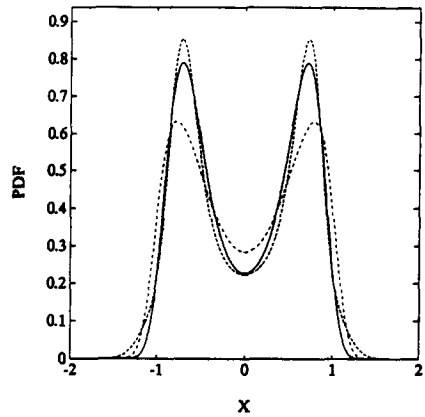

FIG. 7. Steady-state pdfs for $\alpha = -1$, $\beta = 2$, and $D_w = 0.1$ (one-dimensional interpolation between pdfs in Figure 5). Solid: Exact pdf, Dashed: Approximate pdf using (6), Dash-dot: Approximate pdf using (7).

Figure 5. Even though both of those have the same mean $\mu = 0$, the simplified formula leads to a rather inaccurate approximation around the peaks and in the trough. In contrast, both approximate pdfs in Figure 8 are very close to the exact pdf. These approximations have been obtained by interpolating between the pdfs shown in Figure 6; as those do not differ as much as their counterparts in Figure 5, the resulting interpolation is naturally more accurate.

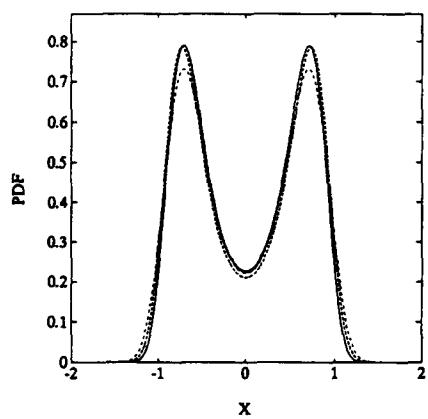

FIG. 8. Steady-state pdfs for $\alpha = -1$, $\beta = 2$, and $D_w = 0.1$ (one-dimensional interpolation between pdfs in Figure 6). Solid: Exact pdf, Dashed: Approximate pdf using (6), Dash-dot: Approximate pdf using (7).

Figures 9 and 10 show the results of interpolating simultaneously in the parameters α and β—a two-dimensional interpolation. In the case of Figure 9, the nodal values are the same as those used in Figures 7 and 8. It is seen that the simplified formula is not very accurate under these circumstances, while (34) gives decent results. For Figure 10, the separation of the nodal values has been halved: α is now interpolated between -0.75 and -1.25, and β is interpolated between 1.75 and 2.25. Shown as dotted curves are two "diametrically opposed" nodal pdfs, one for $\alpha = -0.75$ and $\beta = 1.75$, and the other for $\alpha = -1.25$ and $\beta = 2.25$. There are two other nodal pdfs that are not shown in the figure. As usual, the solid curve is the exact pdf for $\alpha = -1$ and $\beta = 2$, and the dashed curve, now very close to the exact one, is the approximation using (34). The approximation using (35) is not shown but is also quite good, due to the smaller nodal separation.

5.2 Application to Probability Mass Functions

The method is now applied to transient pmfs of the above system that have been obtained through Monte Carlo simulation. To this end, the interval between -2 and 2 in the x coordinate is divided into 40 cells of equal size, and an ensemble of n_e system trajectories is generated starting from a given initial condition x_i. Numerical integrations are carried out to a chosen time t_f. Then, the number of final states in each cell is determined and divided by n_e to yield an estimate of the overall pmf. It can be seen that x_i and t_f may be regarded as interpolation parameters in this scenario. The other parameters α, β, and D_w are kept fixed for the present purposes. Shown in Figure 11 are two pmfs corresponding to $t_f = 0.5$ that have been

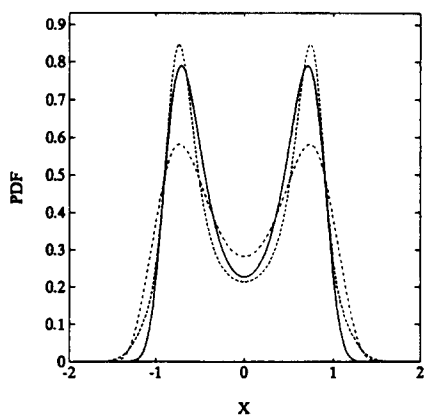

FIG. 9. Steady-state pdfs for $\alpha = -1$, $\beta = 2$, and $D_w = 0.1$ (two-dimensional interpolation). Solid: Exact pdf, Dashed: Approximate pdf using (6), Dash-dot: Approximate pdf using (7).

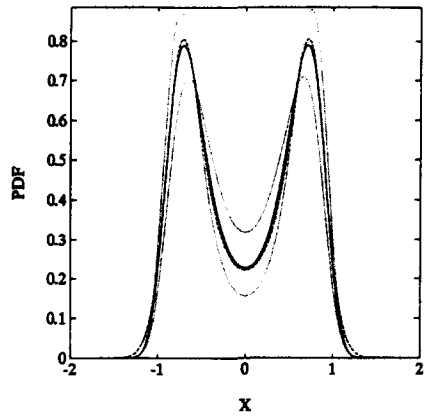

FIG. 10. Steady-state pdfs for $\alpha = -1$, $\beta = 2$, and $D_w = 0.1$ (two-dimensional interpolation with finer mesh). Dotted: Two of the four nodal pmfs, Solid: Exact pdf, Dashed: Approximate pdf using (6).

obtained through Monte Carlo simulation with $n_e = 1500$. The solid curve and the dashed curve correspond to $x_i = 0$ and $x_i = 0.5$, respectively. The former appears symmetric about its mean, while the latter exhibits a "tail" on the left, indicating a drainage of probability into the potential well of the equilibrium at $x = -\sqrt{\alpha/\beta}$. (As $t \to \infty$, both pmfs should assume a bimodal, symmetric shape like the pdfs of Figures 5–10.) Similarly, in Figure 12, two pmfs for fixed $x_i = 0.25$ are shown; the solid curve corresponds to $t_f = 0.25$, while the dashed curve corresponds to $t_f = 0.75$.

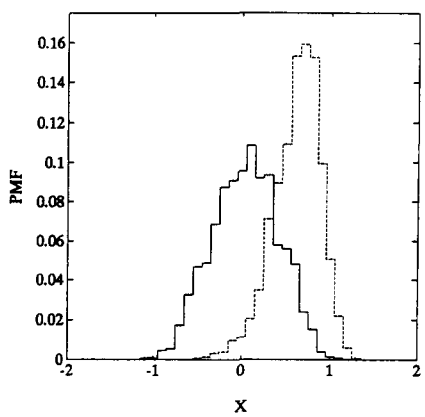

FIG. 11. Pmfs obtained through Monte Carlo simulation with 1500 samples for $\alpha = -1$, $\beta = 2$, $D_w = 0.1$ and $t_f = 0.5$. Solid: $x_i = 0$, Dashed: $x_i = 0.5$.

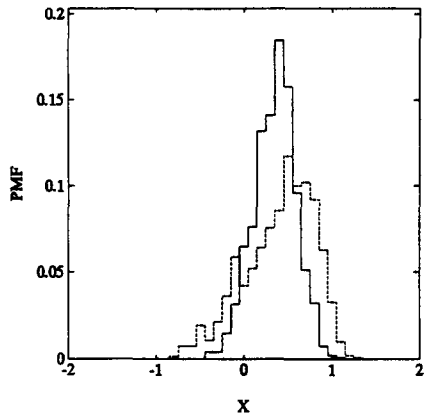

FIG. 12. Pmfs obtained through Monte Carlo simulation with 1500 samples for $\alpha = -1$, $\beta = 2$, $D_w = 0.1$ and $x_i = 0.25$. Solid: $t_f = 0.25$, Dashed: $t_f = 0.75$.

It is possible to interpolate between the pmfs in either set in order to compute an approximation to the pmf for $x_i = 0.25$ and $t_f = 0.5$. Figure 13 shows the result of interpolating in both coordinates simultaneously, using 4 nodal pmfs for which x_i is 0 or 0.5, and t_f is 0.25 or 0.75. The stairstep plot format has been avoided for the sake of clarity. The solid curve is the pmf obtained by a Monte Carlo simulation with $n_e = 1500$, while the dashed and dash-dot curves are the pmfs found by proper (51) and simplified (53) interpolation. Qualitatively, the same trends that were observed in the case

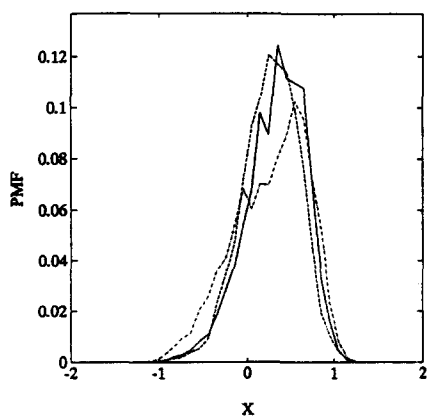

FIG. 13. Pmfs for $\alpha = -1$, $\beta = 2$, $D_w = 0.1$, $t_f = 0.5$, and $x_i = 0.25$. Solid: Pmf obtained through Monte Carlo simulation with 1500 samples, Dashed: Approximate pmf using (22), Dash-dot: Approximate pmf using (24).

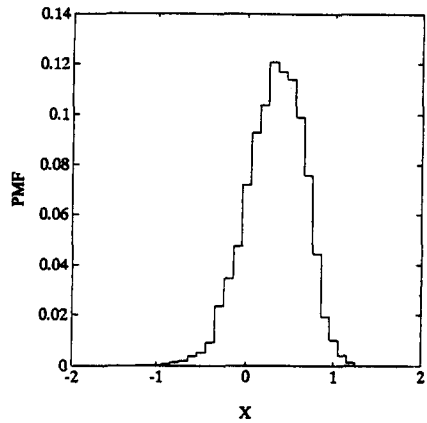

FIG. 14. Stairstep plot of approximate pmf using (22).

of pdfs are discernible in this case, as well: The simplified interpolation is less accurate (but becomes acceptable when nodal separation is decreased), and the proper interpolation essentially has the correct shape, with a slight shift in the mean. Furthermore, it can be seen from the plot (and verified through further testing) that interpolation between pmfs obtained through simulation has the additional benefit of reducing the "jaggedness." This may also be appreciated by comparing the stairstep plot of the properly interpolated pmf, given as Figure 14, to the simulated pmfs shown in Figures 11 and 12.

All of the above studies have been performed using MATLAB on an IBM Personal System/2 computer. While no attempt at particularly efficient formulations has been made, it is instructive to compare the operation counts involved in interpolation versus simulation. For $n_e = 1500$ as in the examples in Figures 11–13, on the order of 650k floating point operations (fpo) are required for each pmf found by Monte Carlo simulation. This number scales essentially linearly with n_e. In contrast, the effort involved in obtaining pmfs through interpolation depends only on the number of cells; for 40 cells as shown in Figures 13 and 14, around 22k fpo are performed for the proper interpolation and less than 1k fpo for the simplified interpolation. Thus, significant savings in computational effort are realized relative to simulation. In the case of pmfs, computing the volume fractions γ_{jk} is the most intensive part of the interpolation and can be made more efficient by various means, such as computing γ_{jk} only for those values of k that have nonzero $P(k)$, or approximating the volume fraction by considering test points as described in Section 4.4. Significant savings are also possible in the case of a reasonably fine grid of cells by viewing the pmf as an approximation to a pdf and using the continuous interpolation formula (34). Splines or

even linear interpolation between pmf values in adjacent cells may be used in this regard. Attempts at additional efficiency along these directions have not been made in this preliminary study.

6. CONCLUSIONS

Formulas for interpolating between probability density and mass functions in spaces of arbitrary dimensionality have been developed and applied to sample problems. It is found that these formulas give accurate results even when the functions one is interpolating between are not that "close," i.e., when the nodal separation in the parameter space is relatively large. Naturally, as the mesh used in interpolation is refined, the accuracy of the interpolated quantities increases. Thus, in addition to the more complicated and robust interpolation formulas meant for the case of a coarse mesh, simplified versions are given that result in good accuracy when the mesh is fine. Even when the more complicated interpolation formulas are used, savings in computational effort up to a factor of one hundred are common. This means that interpolation is a lucrative alternative to Monte Carlo simulation and even to the Generalized Cell Mapping (GCM) method when the complete probability distribution, as opposed to only the low-order statistics, is needed.

Using interpolation, one may account for the effects that changing parameters (be they material constants, initial conditions, or time) have on the resulting probability distribution. This is different from straightforward numerical interpolation because one is interpolating between entire functions, as opposed to between numbers. Viewed from that perspective, the formulas given may also be interpreted as general-purpose algorithms for the blending of shapes and may have applications beyond what is considered in this paper. Further work is needed to explore that possibility and to apply the development in this paper to some probability distributions arising from real-world applications.

REFERENCES

1 T. T. Soong, *Random Differential Equations in Science and Engineering*, Academic Press, New York, 1973.

2 Y. K. Lin, *Probabilistic Theory of Structural Mechanics*, reprint edition with corrections, Krieger, New York, 1976.

3 S. H. Crandall and W. Q. Zhu, Random vibration: A survey of recent developments, *ASME J. Appl. Mech.* 50:953–962 (1983).

4 R. A. Ibrahim, *Parametric Random Vibration*, Research Studies Press Ltd., U.K., 1985.

5 L. A. Zadeh, Fuzzy sets, *Inform. and Control.* 8:338–353 (1965).

6 D. Dubois and H. Prade, *Fuzzy Sets and Systems: Theory and Applications*, Academic Press, New York, 1980.
7 R. H. Toland and C. Y. Yang, Random walk model for first-passage probability, *ASCE J. Eng. Mech. Div.* 97:791–807 (1971).
8 J. B. Roberts, First passage time for randomly excited nonlinear oscillators, *J. Sound Vib.* 109(1):33–50 (1986).
9 W. F. Wu and Y. K. Lin, Cumulant-neglect closure for nonlinear oscillators under parametric and external excitations, *Int. J. Non-Linear Mech.* 9(4):349–362 (1984).
10 C. S. Hsu, *Cell-to-Cell Mapping: A Method of Global Analysis for Nonlinear Systems*, Springer-Verlag, New York, 1987.
11 C. S. Hsu and H. M. Chiu, A cell mapping method for nonlinear deterministic and stochastic systems—Part I: The method of analysis, *ASME J. Appl. Mech.* 53:695–701 (1986).
12 H. M. Chiu and C. S. Hsu, A cell mapping method for nonlinear deterministic and stochastic systems—Part II: Examples of application, *ASME J. Appl. Mech.* 53:702–710 (1986).
13 J. Q. Sun and C. S. Hsu, A statistical study of Generalized Cell Mapping, *ASME J. Appl. Mech.* 54:649–655 (1987).
14 J. Q. Sun and C. S. Hsu, First-passage time probability of nonlinear stochastic systems by the Generalized Cell Mapping method, *J. Sound Vib.* 124(2):233–248 (1988).
15 J. Q. Sun and C. S. Hsu, The Generalized Cell Mapping method in nonlinear random vibration based upon short-time Gaussian approximation, *ASME J. Appl. Mech.* 57:1018–1025 (1990).
16 F. H. Bursal, Efficient simulation of systems with random uncertainty using interpolation, in *Proceedings of the 28th Annual Simulation Symposium*, IEEE Computer Society Press, Los Alamitos, CA, 1995, p. 259–267.
17 D. P. Ahlfeld and G. F. Pinder, A fast and accurate method for solving subsurface contaminant transport problems with a single uncertain parameter, *Adv. Water Resources* 15:143–150 (1992).
18 M. Segev and J. Stepanek, Probabilities for lattice integral transport, *Nucl. Sci. Eng.* 108:208–213 (1991).
19 E. G. Coffman, B. M. Igelnik, and Y. A. Kogan, Controlled stochastic model of a communication system with multiple sources, *IEEE Trans. Info. Th.* 37(5): 1379–1387 (1991).
20 T. Misawa, Reaction probability derived from a stochastic interpolation formula, *Phys. Lett. A.* 179:385–388 (1993).
21 G. Strang and G. Fix, *An Analysis of the Finite Element Method*, Prentice-Hall, Englewood Cliffs, NJ, 1973.
22 B. H. Tongue and K. Gu, A higher order method of Interpolated Cell Mapping, *J. Sound Vib.* 125(1):169–179 (1988).
23 N. Wiener, Differential space, *J. Math. Phys.* 2:386–394 (1923).
24 N. C. Nigam, *Introduction to Random Vibrations*, The MIT Press, Cambridge, MA, 1983.